*Geophys. J. Int.* (2004) **158,** 712–728 doi: 10.1111/j.1365-246X.2004.02279.x

# Geoelectric structure of the Dharwar Craton from magnetotelluric studies: Archean suture identified along the Chitradurga–Gadag schist belt

S. G. Gokarn, G. Gupta and C. K. Rao

*Indian Institute of Geomagnetism, Plot* 5, *Sector* 18, *Kalamboli, New Panvel (West) Navi Mumbai,* 410 218, *India. E-mail: gokarn@iigs.iigm.res.in*

Accepted 2004 February 6. Received 2004 February 5; in original form 2002 April 18

## SUMMARY

Broad-band magnetotelluric data were collected at 50 stations over a 400 km long, approximately east–west profile over the granite–greenstone terrain of Dharwar, southern India. The tensor decomposed data were interpreted using a 2-D inversion scheme. The geoelectric model is suggestive of a suture along the Chitradurga–Gadag schist belt, formed by the thrusting of the West Dharwar Craton beneath its eastern counterpart, with an easterly dip of 20–30°. The thrust proposed here pre-dates the formation of these schists, which occurred during the Late Archean (2600 Ma). The accretionary wedge of the thrust and the depressed part of the West Dharwar Craton may have controlled the emplacement of the Chitradurga–Gadag and Shimoga–Dharwar schists. The subsequent weathering, the several episodes of tectonic activity witnessed during the Precambrian and the vertical block movements caused during the passage of the Indian Plate over the Reunion hotspot may have modified the crust, leading to the present-day geological configuration. Despite its age and several tectonothermal episodes, the signature of this thrust is adequately preserved in the Dharwar Craton. Several similarities with younger sutures, as is evident from the observed relics of the oceanic rocks present along the Chitradurga schist belt, suggest that the tectonic processes leading to this Archean event may have had a close resemblance to those witnessed in recent times. Magnetotelluric studies also image a zone of low resistivity at a depth of 40 km beneath the west Dharwar Craton. This seems to be a regional feature, extending to the north over a distance of at least 250 km beneath the Deccan volcanics. The low heat flow values and the high density associated with this feature make partial melting an unlikely explanation for the low resistivity. The grain boundary graphites and the sulphides deposited in the form of pyrites may have caused the low resistivity in the lithospheric mantle of the West Dharwar Craton, although the fluids generated and trapped in the mantle during the passage of the Indian Plate over the Reunion hotspot in the waning phase of its outburst could also be a possibility. The asthenosphere is delineated at a depth of about 100 km beneath the East Dharwar Craton.

**Key words:** Archean suture, Archean tectonics, Dharwar Craton, magnetotellurics, South Indian Shield.



## 1 INTRODUCTION

The South Indian Shield forms a coherent unit in which geological activity can be traced continuously over the entire Precambrian. It records more than a billion years of the early history of the Earth, involving several episodes of crustal development. The Dharwar Craton is located in the central part of the South Indian Shield, flanked by the high-grade granulitic terrain to the south and the younger cover of the Deccan flood basalts to the north (Fig. 1). Almost the entire craton is covered by the Tonalitic Trondjhemitic gneisses (termed the Peninsular gneisses) with several northwest–southeast trending schist belts and intrusive granites. All the rocks in the Dharwar Craton are Archean to Late Proterozoic in age (Radhakrishna & Naqvi 1986). The structural patterns have been modified by three tectonothermal events that occurred between 3400 and 2500 Ma (Mukhopadhyay 1986). Their signatures are well preserved despite the Palaeozoic pan-African deformations of the East Gondwana Block (Boger *et al.* 2002), in which the Indian Plate was involved. These include the Cretaceous outburst of the Reunion hotspot and the subsequent eruption of the Deccan volcanics in the northern part of the Dharwar Craton (Raval & Veeraswamy 2000). This craton thus provides an ideal setting for studying the tectonothermal

 

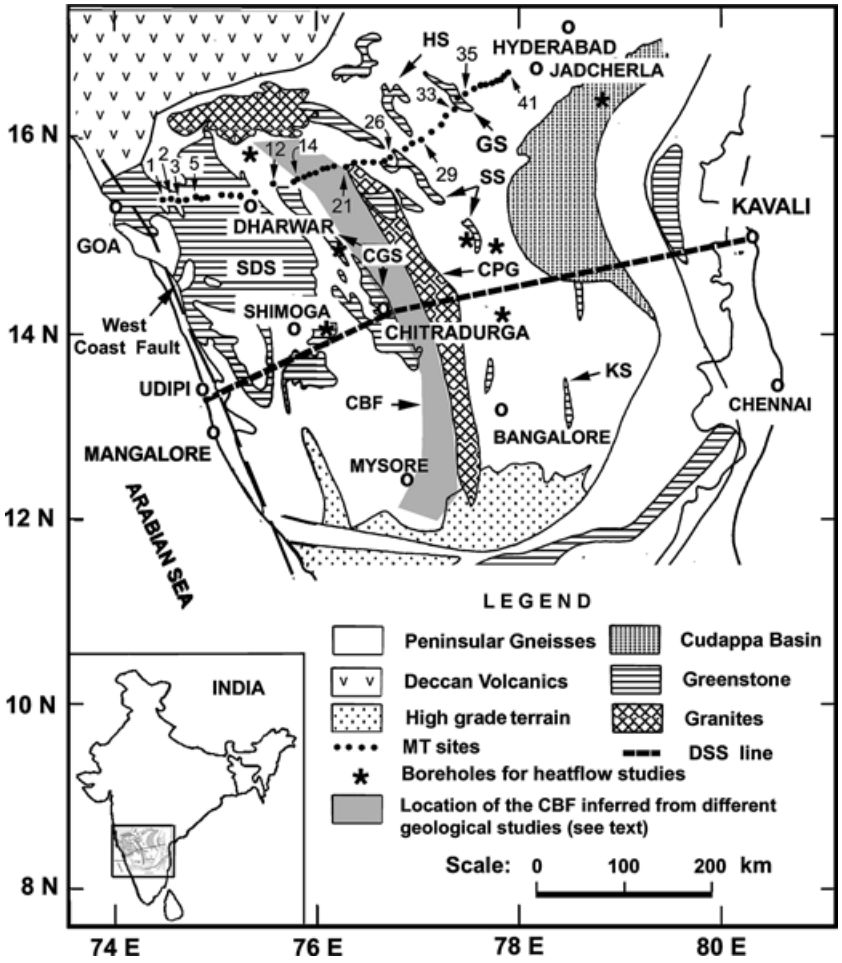


**Figure 1.** Geological map of the South Indian Shield showing the locations of the MT stations. For the sake of clarity only some stations are numbered. Also shown here are the locations of the boreholes used for heat flow studies (Roy & Rao 2000) and the location of the DSS profile (Kaila *et al.* 1979): SDS, Shimoga Dharwar schists; CGS, Chitradurga–Gadag schists; CPG, Closepet granites; KS, Kolar schists; SS, Sandur schists; HS, Hutti schists; GS, Gadwal schists. CBF: positions of the Chitradurga Boundary Fault as expected from different geological studies are located in the grey shaded region (see text for detailed description).

processes which were active during the Archean and the Precambrian. Despite geological studies conducted over the past 150 yr, there is no unanimity of opinion on the stratigraphy and the crustal evolutionary processes in this region. The major controversy is centred around the schist–gneiss relationship (Radhakrishna & Naqvi 1986). However, it is generally believed that the emplacement of the gneisses and the mafic volcanics occurred during the Early Archean, followed by the deposition of the younger schist belts and the intrusion of the potassium-rich granites in the Late Archean. Early geophysical studies in this region were limited to regional gravity studies, some limited heat flow studies and a deep seismic sounding profile across the Dharwar Craton. In recent times, several parts of the South Indian Shield have been actively probed by different geophysical methods.

The present work is an effort towards delineating the electrical structure of the crust and mantle beneath the Dharwar Craton by using the magnetotelluric (MT) technique, which may be of significance in furthering our knowledge of the crustal evolutionary processes active during the Archean. In view of the predominantly northwest–southeast tectonic fabric evident in the geology (Fig. 1) an approximately ENE–WSW trending profile between Goa–Dharwar–Jadcherla, perpendicular to the tectonic fabric, was chosen for the study here.

## 2 GEOLOGY AND TECTONICS

A geological map of the Dharwar Craton is shown in Fig. 1 along with the location of the MT sites. Also shown here are some of the boreholes used for the heat flow studies (Gupta *et al.* 1991; Roy & Rao 2000) pertinent to the discussion here and the location of the profile covered by deep seismic sounding studies (Kaila *et al.* 1979). The entire Dharwar Craton can be viewed as a matrix of Peninsular gneisses interspersed with high- and low-grade schist belts and the intrusive granites. The Shimoga–Dharwar (SDS) schist belt with a maximum width of 150 km, in the western part of the craton, is the most prominent schist, followed to the east by the Chitradurga–Gadag schists (CGS) and several narrow discontinuous belts such as the Sandur schists (SS), Hutti schists (HS), Kolar schists (KS), Gadwal schists (GS), etc. The CGS and SDS are younger schist belts deposited in the Late Archean (2600 Ma) whereas, the SS, HS, GS and KS are older and have metamorphosed to high-grade amphibolite to granulite facies (Radhakrishna & Naqvi 1986). The

intrusion of the Closepet granites (CPG) is known to have occurred around 2600–2000 Ma (Radhakrishna 1984).

Based on the differences in the metamorphic facies of the schist belts, their relationship with the surrounding gneisses and some limited geochronological data, this craton is divided in to the east and west Dharwar blocks. Several differences between these two blocks are listed in Ramam & Murty (1997). Perhaps the most obvious difference from the geophysical view point is the distribution of the schist belts, which are narrow, to the extent of becoming discrete patches in the East Dharwar Block whereas in the western block, SDS and CGS are wide and continuous. The gneisses in west Dharwar are dated at 3000–2600 Ma with some areas of 3300 Ma, and show a kaynite–silliminite metamorphism, whereas the eastern block mainly consists of relatively younger gneisses dated at 2600 Ma. Furthermore, several granitic intrusives dot the east Dharwar crust, among which the Closepet granites are the most prominent. There are very few granitic intrusions in the western block. Based on these differences a major tectonic divide along the Chitradurga–Gadag schist belt, known as the Chitradurga Boundary Fault, is proposed. Difference of opinion exist over the location of this fault, although there is general agreement over the importance of this feature in the evolution of the Dharwar Craton. In view of these differences, the location of the Chitradurga Boundary Fault is shown as a grey band in Fig. 1. Several pieces of geological evidence, such as the presence of the recumbent fold belts and thrusts (Kaila *et al.* 1979), crustal shortening as indicated by the folds, consistent east-dipping axial schistocity, and the presence of deep-water marine sediments such as greywackes, oceanic tholeiites, komatites and intermediate acid volcanics and bedded sulphides along Chitradurga Gadag schists, led Radhakrishna & Naqvi (1986) to suggest that the Chitradurga Boundary Fault may be an Archean suture located along the Chitradurga–Gadag schist belts. On the basis of geochronological and geochemical considerations, however, Swami Nath *et al.* (1976) and Narayanaswami (1975) believe that the Chitradurga Boundary Fault is located along the western margin of the Closepet granites.

In recent times, several geophysical studies have been undertaken over the Dharwar Craton and some results are available. Studies of regional gravity, a deep seismic sounding profile and heat flow were conducted much earlier. Several scientists have used these results to obtain substructural information. A Bouguer gravity map of the granite greenstone region is shown in Fig. 2. Qureshy *et al.* (1967) have noted that the gravity highs in this region are located over the schist belts and the moderate gravity lows are associated with the exposures of the granites and gneisses. From studies of Bouguer gravity anomalies over the entire granite–greenstone province, Subrahmanyam & Verma (1982) observed that the regional trends in gravity are oriented predominantly along north–south and NNE–SSW axes. Based on the regional gravity trend determined from $1^\circ \times 1^\circ$ averaged gravity values, these authors propose that the crust on the western part of the Dharwar Craton may be thicker than to the east of the Chitradurga Boundary Fault.

Deep seismic sounding (DSS) studies have been conducted over the east–west profile between Kavali and Udipi (Fig. 1), cutting across the entire width of the Indian Peninsula (Kaila *et al.* 1979). This profile is located about 200 km to the south of the MT profile, but the geological setting is similar to that in the present study area. The seismic reflections obtained from the deep seismic sounding studies over the part of this profile relevant to the discussion here are shown in Fig. 8 along with the deep geoelectric cross-section, to be described later. These are also shown, superimposed over the geoelectric cross-section in Fig. 10. The Moho is delineated at depth

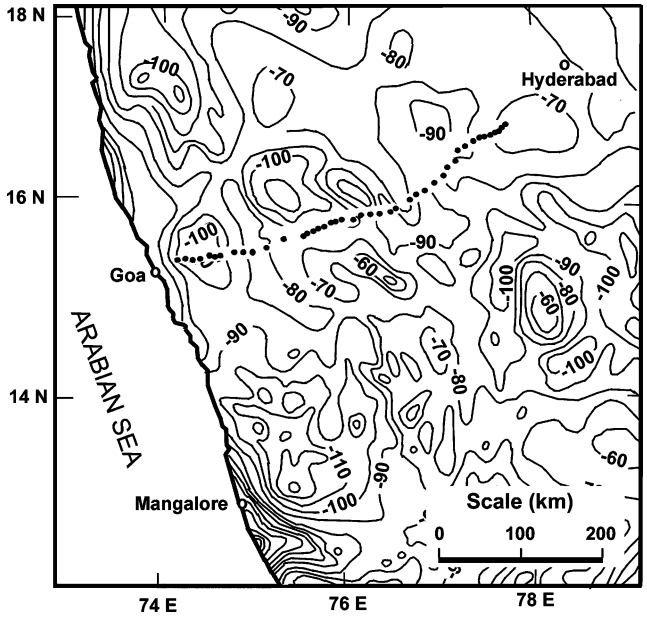


**Figure 2.** Bouguer gravity map of the granite–greenstone belt in the South Indian Shield. The MT stations are marked by solid circles.

of 34 km beneath the Chitradurga schist belts, and on the west the depth to this discontinuity increases to about 41 km. Further west the Moho flattens at shallower depth of 38 km. This observation indicates a moderate thickening of the crust to the west of Chitradurga–Gadag schists. The Moho is not present in the region corresponding to the Closepet granites. It may be pertinent to note here that the Moho is delineated by Kaila *et al.* (1979) as the strongest reflection from reversed traveltime data from the reciprocal shot points. Due to the unavailability of such reciprocal coverage beneath the Closepet granites, the Moho is not shown in this region. Another synclinal feature is evident in the seismic reflections, as well as the thickening of the Moho, to the immediate east of the Closepet granites (beneath stations 25 and 26 in Fig. 10). Several fold belts are observed in the reflectivity pattern throughout the DSS study area, indicative of the regional-level compressional tectonics over the entire width of the Indian Peninsula. The teleseismic studies (Gupta *et al.* 2003) report much thicker crust (42–51 km) beneath the West Dharwar Craton.

Srinagesh & Rai (1996) observe that the seismic velocities at a depth of 40–180 km, corresponding to the upper mantle, are higher in the western block than those in the eastern block by about 2–3 per cent. The mantle at depths greater than 180 km, however, does not show any systematic trend in the seismic velocities.

From the borehole studies, Roy & Rao (2000) and Gupta *et al.* (1991) have observed that the surface heat flows are higher in the East Dharwar Block (they vary in the range of 36–47 mW $m^{-2}$, with an average value of 40 mW $m^{-2}$) than the values of 28–37 mW $m^{-2}$ (average: 31 mW $m^{-2}$) observed in the West Dharwar Block. The thickness of the lithosphere estimated from these studies is more than 200 km. Gupta *et al.* (1991) have further observed that the gneisses beneath west Dharwar are mainly tonalitic, whereas those to the east are dotted with several granitic intrusives. These authors suggest that different magmatic processes may have been active in the crustal blocks of east and west Dharwar.

The crustal evolution of the South Indian Shield may have been influenced by the Early Palaeozoic pan-African orogenic activity (Boger *et al.* 2002) in which the Indian Plate, then a part of the East Gondwana Block, was involved and also the hotspot activity of

the Marion and Reunion hotspots during the Late Cretaceous. The outburst of the Marion hotspot caused the break-up of Madagascar from the Indian continent (Kumar *et al.* 2001). The outburst of the Reunion hotspot at 65.5 Ma (Raval & Veeraswamy 2000) caused widespread fissure eruption of the Deccan flood basalts, about 30–100 km to the north of the present study area (Cox 1989). Several vertical movements are witnessed along the west coast in the Deccan basaltic province as well as the Dharwar Craton caused by the Reunion hotspot during the transit of the Indian Plate over it, loading of the flood basalts as well as the subsequent erosional activity.

## 3 DATA COLLECTION AND ANALYSIS

Magnetotelluric data were collected at 50 stations over the 400 km long ENE–WSW trending Goa–Dharwar–Jadcherla profile, shown in Fig. 1. Data were collected in the frequency range 320–0.0005 Hz using two V-5 MT systems manufactured by Phoenix Geophysics, Canada. The high crustal resistivities of the Archean rocks lead to large-scale spreading of the electromagnetic noise caused by farming activities and boreholes. Thus the data collection was a tedious process and several stations had to be relocated to obtain acceptable data quality. Of the 50 stations surveyed, seven were rather noisy and were not used for further interpretation. Data were analysed using the single-site robust estimation procedure, which is a combination of fast Fourier transforms and a cascade decimation technique for obtaining the auto- and cross-power spectra required for computing the frequency variation of the apparent resistivity and phase of the impedance (Wight & Bostick 1980).

The impedance tensors at the 43 stations were decomposed using the tensor decomposition procedure of Groom & Bailey (1989), using the step-by-step approach described by Groom *et al.* (1993). The unconstrained decomposition at individual frequencies indicated that the shear had a stable value at most frequencies at most of the stations. The shear was then constrained to its median value and the decomposition procedure was repeated with unconstrained twist and strike angles. This resulted in a marked improvement in the stability of the twist and the strike angles. The twist was then varied in the vicinity of its median value to further decrease the frequency dependence of the observed strike angles. The average strike directions at low frequencies (<0.1 Hz) at all stations are shown in Fig. 3 (after correcting for 90° ambiguity). Most of the stations show a strike angle of N45°W within about 10°, indicating a predominantly 2-D geoelectric structure with a regional strike along an approximately northwesterly direction. The high-frequency strike directions were influenced by the topsoil cover, which consists of black cotton and laterite soils, occurring in discrete patches in this resistive Archean terrain. Since our interest here lies in the deeper features, the strike angles at lower frequencies (<0.1 Hz) are considered.

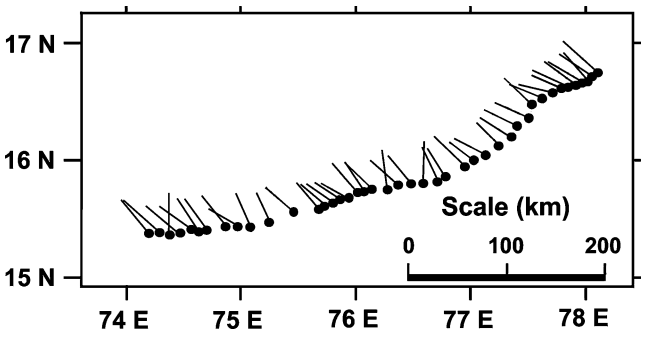


**Figure 3.** Average Groom–Bailey strike angles at low frequencies (0.01–0.001 Hz).

In order to further constrain the regional strike, the impedance tensors at all the stations were decomposed using the multistation, multifrequency tensor decomposition scheme of McNeice & Jones (2001) wherein the apparent resistivity and phase data at all stations and frequencies were simultaneously decomposed. The RMS misfits of the 3-D/2-D decomposition model to the observed data are shown in Fig. 4(c). Here the crosses denote the values which were removed as outliers and the open circles denote those values with misfit of more than 16 and which were thus removed after the multisite, multifrequency decomposition. Also shown here are the shear and twists at the individual stations (Figs 4a and b). Generally the RMS misfits are in the range of 2–8. Some high values for the RMS misfit are observed at frequencies higher than 50 Hz, which may be due to the inductive distortions caused by the heterogeneous topsoil cover. As mentioned earlier, the topsoil consists of black cotton soil and red laterite soil, occurring in patches, especially in the central part of the profile, between stations 12 and 33. The shear and twist angles are less than 15° at most of the stations. These observations suggest that the geoelectric structure in the survey region fits well with the 3-D/2-D approximation, with a regional strike angle along N42.6°W or perpendicular to it (due to the 90° ambiguity). The responses corrected for the distortions were used for further interpretation.

The geological and tectonic features are predominantly along the north–south to northwest–southeast directions in general and have a northwest–southeast orientation in the MT survey region. The northwest–southeast tectonic fabric of the study area is also clearly indicated in the magnetic susceptibility map of the Dharwar region obtained using the aeromagnetic anomalies (Harikumar *et al.* 2000). In view of these observations, the regional strike direction was chosen to be N42.6°W. The response functions associated with the electric field parallel to this direction are regarded as the TE-mode values and those with the electric field measured perpendicular to it, the TM-mode values. All the stations were projected on a straight line perpendicular to the regional strike before proceeding further with the interpretation.

The study area is located in the close proximity of the Arabian Sea, which is about 30 km away from station 1 on the western end of the profile. The bathymetry of the Arabian Sea off the coast of Goa is shown in Fig. 6, along with the grid structure used for invoking the sea in to the 2-D model, to be discussed later. The west coast is aligned approximately along N25°W, which is different from the geoelectric strike observed here. The strike angles at the stations in the close vicinity of the coast do not show any significant influence of the coast, indicating that the MT responses may not be affected by the coast effect. A quantitative discussion on this aspect will be made later while discussing the sensitivity of the observed features in the Section 5, on 2-D modelling.

## 4 STATIC SHIFT CONSIDERATIONS

The apparent resistivity and phase pseudo-sections of the observed responses are shown in Figs 5(a) and (b) respectively. The forward-modelled responses, computed for the geoelectric cross-section to be discussed in the next section, are also shown here. As mentioned earlier, the topsoil in the survey region comprises the red laterite soil and black cotton soil, occurring in patches throughout the MT survey profile. Normally the black cotton soil is highly conductive whereas, the red laterite soil tends to be more resistive, thus causing

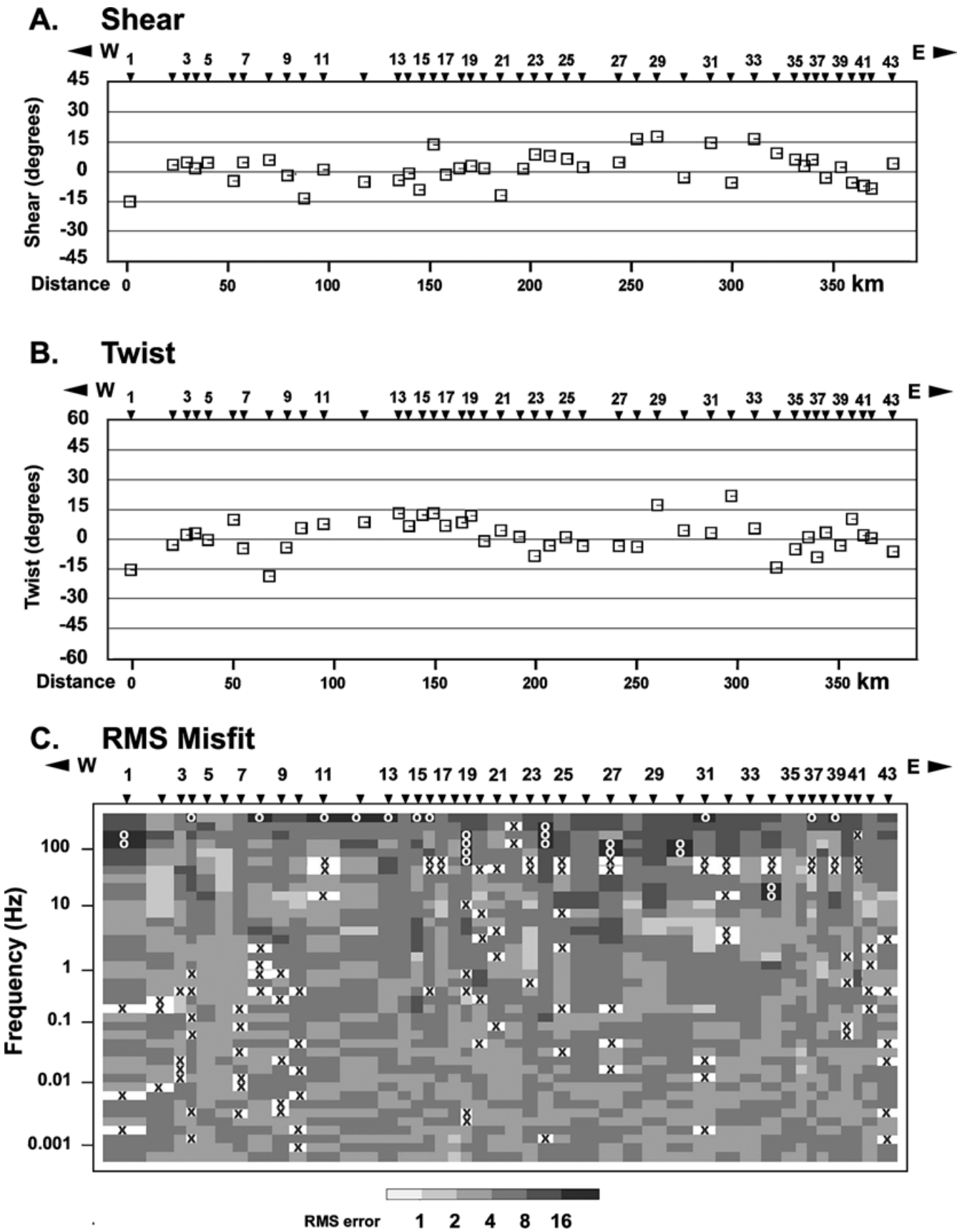


**Figure 4.** Spatial variation of the (A) shear, (B) twist and (C) rms misfits obtained using the multisite, multifrequency tensor decomposition. The circles in (C) denote rms misfit values of more than 8 and the crosses are the outliers. These points were not included in the inversion.

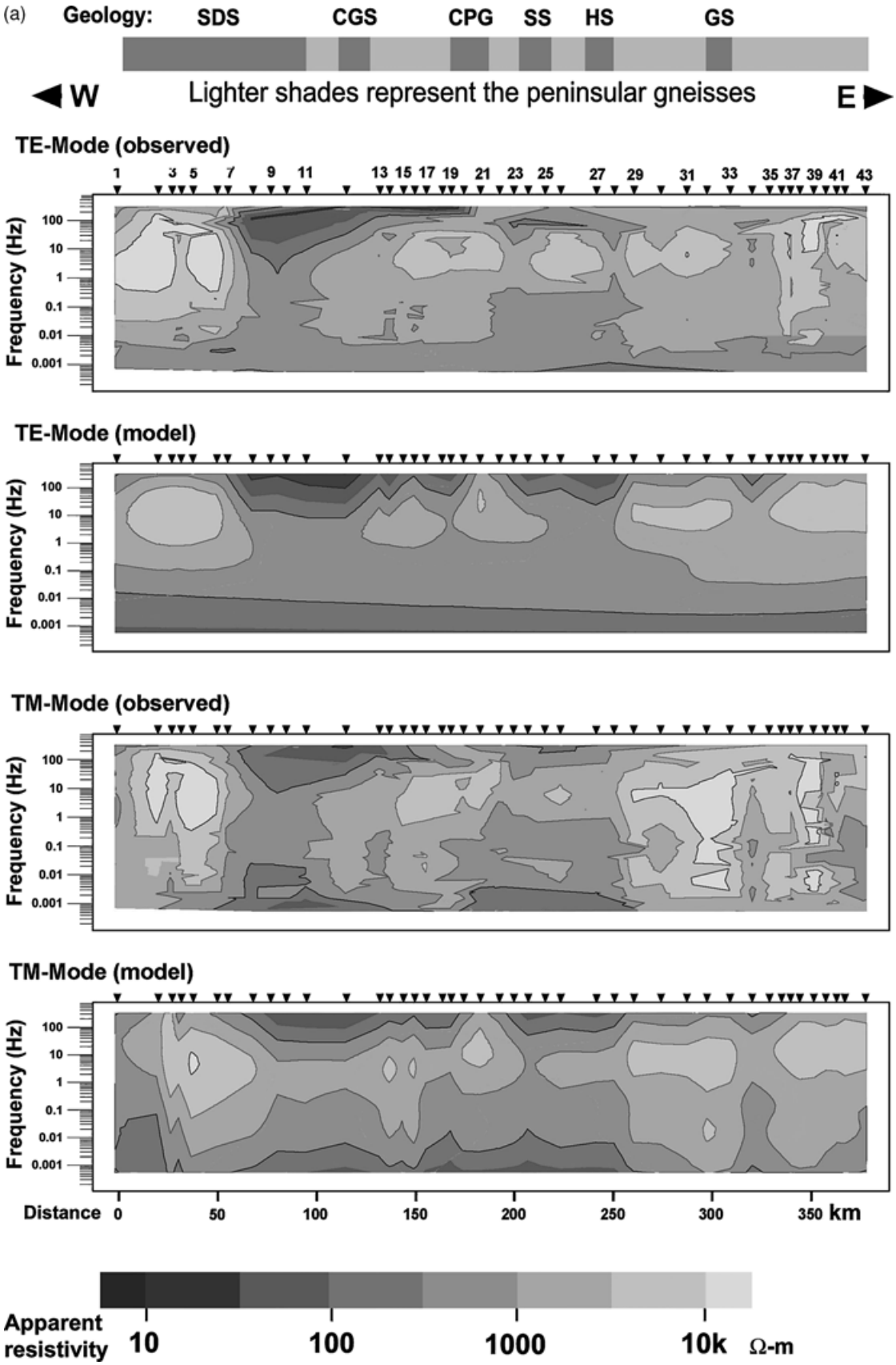


**Figure 5.** (a) Observed and modelled apparent resistivity pseudo-sections in TE and TM modes. Only alternate stations are numbered here for the sake of clarity. Data at all stations are used for the interpretation. SDS, Shimoga–Dharwar schists; CGS, Chitradurga–Gadag schists; CPG, Closepet granites; SS, Sandur schists; HS, Hutti schists; GS, Gadwal schists. (b) Observed and modelled phase pseudo-sections in TE and TM modes. Only the alternate stations are numbered here for the sake of clarity. Data at all stations are used for the interpretation. Key as for (a).

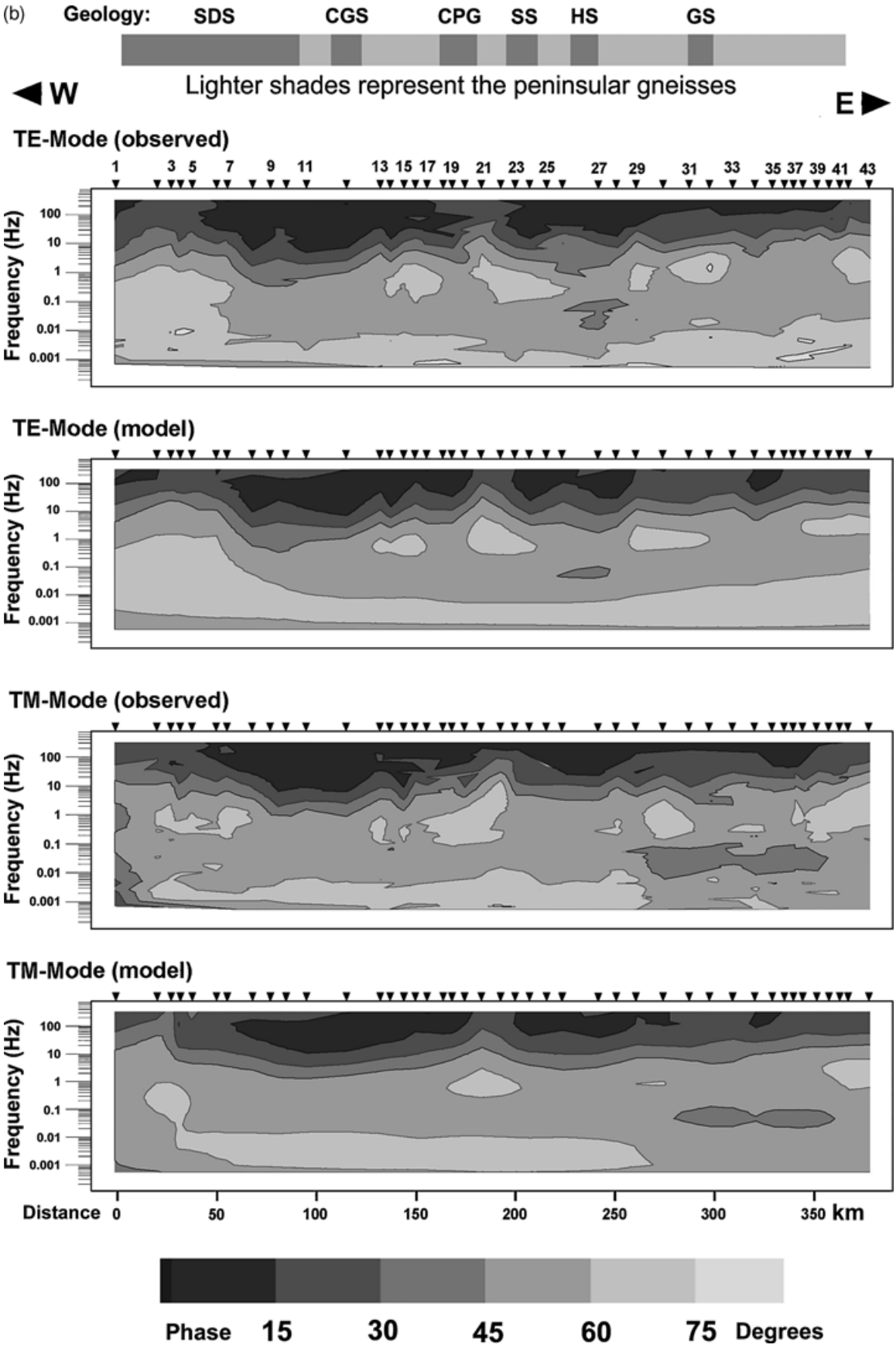


**Figure 5.** *Continued.*

severe resistivity inhomogeneities at the surface. The static shifts are generally corrected by constraining some of the model parameters using the inputs from other geophysical studies. However, no such details are available in the present study area. In such cases, the apparent resistivities at low frequencies are spatially filtered to a low-order polynomial and the TE apparent resistivity curves are shifted vertically on the logarithmic scale so as to coincide with the smoothed response at low frequencies (Jones & Dumas 1993). The assumption here is that the deep geoelectric structure is laterally uniform.

The phases which are not influenced by the shallow inhomogeneities show some spatial variations at low frequencies ($<$0.01 Hz), indicating the possible 2-D features at deep levels, and thus even the second approach may not be suitable for the purpose of static shift correction. Thus static shifts were not corrected here. In order to circumvent the problem of distortion due to shallow inhomogeneities, the influence of the apparent resistivities on the geoelectric model was decreased by increasing their error bars by a factor of 10. Thus the geoelectric structure is strongly influenced by the phase data, which is free from the static problem. However, the phase data do not contain information on the absolute resistivity values of the substructure. The down-weighted apparent resistivities are useful in constraining these values.

## 5 TWO-DIMENSIONAL INVERSION

Both the TE and TM mode response functions, modified as described earlier, were used for obtaining the geoelectric structure. The starting model was a half-space with a uniform resistivity of 100 Ω m. The study region is in the close vicinity of the Arabian Sea to the west (about 30 km away from the station 1). In the absence of any significant drainage into the Arabian Sea, the water has high salinity and thus a low resistivity of 0.25 Ω m was invoked to the west of the geoelectric model with dimensions conforming to the bathymetry shown in Fig. 6. Here the observed bathymetry (Eremenko & Negi 1968) is shown along with the resistivity structure invoked for the sea in the 2-D model.

The 2-D inversion programme of Rodi & Mackie (2001) was used for obtaining the geoelectric structure. The noise floor and smoothing factor ($\tau$) were set at 5 per cent and 5 respectively. After 200 iterations, root-mean-square (rms) misfit was 1.54. The forward responses for the model thus obtained are shown in Figs 5(a) and (b) along with the observed response function for the sake of comparison. A reasonable agreement exists between the observed and modelled phases (Fig. 5b). However, the agreement between observed and modelled apparent resistivities (Fig. 5a) exists only in a broad sense, with several misfits. As mentioned earlier, the weight of the apparent resistivity was decreased in relation to the phase, and thus large misfits are expected between modelled and observed apparent resistivities. The geoelectric cross-section in the top 25 km is shown in Fig. 7 with a vertical exaggeration of about 5. Also shown here is the Bouguer gravity variation along the MT profile. The deep geoelectric cross-section is shown in Fig. 8 with no vertical exaggeration. The seismic reflectors obtained from the deep seismic sounding studies (Kaila *et al.* 1979) are shown on the top part of this figure.

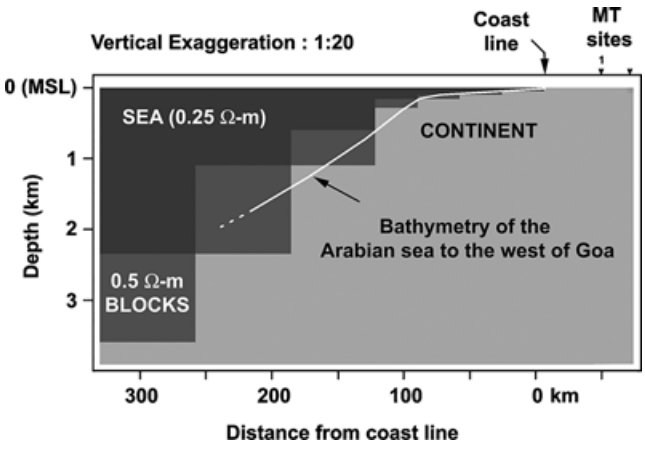


**Figure 6.** Bathymetry of the west coast and adjoining Arabian Sea (solid line) and the grid configuration used for invoking the sea in the 2-D inversion scheme.

## 6 HYPOTHESIS TESTING AND SENSITIVITY

A low-resistivity top layer is indicated in all response functions, in the form of low phase (indicative of a low resistivity at frequencies higher than the highest sounding frequency of 320 Hz) and also the increase of apparent resistivity with decreasing frequency at the high-frequency end (Figs 5a and b). This low-resistivity layer at the top is caused by the topsoil, which comprises the black cotton and the laterite soils occurring as irregularly shaped discrete patches with lateral dimensions of 0.1 to 20 km, extending in depth up to 10–300 m throughout the survey profile. No attempts are made here to show or interpret this layer, because it is a result of weathering and erosional processes which do not have any geophysical significance.

The geoelectric structure is rather complex, with several lateral resistivity contrasts extending in to the lithospheric mantle, and hence for the convenience of the discussion here the major features in Figs 7 and 8 will be referred to by the letters shown in these figures. A high-resistivity layer (A in Figs 7 and 8), having a resistivity of more than 5000 Ω m and a thickness varying between 5 and 40 km, is delineated throughout the survey profile. To the east of station 11 this layer is generally about 5 km thick, with three east-dipping resistive wedges projecting downwards to depth of about 15 km (to be discussed in detail later) whereas, to the west, this layer extends to depth of about 30 km beneath station 2. This high-resistivity layer A is underlain to the east of station 7 by a low-resistivity layer (B in Figs 7 and 8) extending up to a depth of about 20 km and with a conductance of 50–100 S. A high-resistivity layer (C) having a resistivity of 500 Ω m is delineated at depth of about 20 km between stations 11 and 27 in the central part of the profile and has a depth extent of about 40 km. Further east, a high-resistivity body (D) with resistivity of more than 10 000 Ω m is delineated at a lower crustal depth of about 30 km, extending deep in to the mantle to about 160 km. The westward continuation of C beneath stations 7 and 9 is also not very clear and a resistive feature E is marked here beneath stations 8 and 13 (Fig. 8) in the depth range 20–70 km. The features C, D and E are underlain by a low-resistivity feature (F) with a resistivity of about 50 Ω m at a depth of about 80 km and beyond. Strong lateral variations are observed in the geoelectric structure even at this depth, corresponding to the lithospheric mantle. The westward extension of F is not obvious, although the low resistivity seems to rise to a shallow depth of about 50 km to the west, between the stations 2 and 7, but has a much lower resistivity of 20 Ω m and hence this is treated as a distinct feature (G) here, with F continuing beneath G at deeper levels of about 80 km.

Several vertical and subhorizontal resistivity contrasts are observed in the geoelectric section, and hence the sensitivity of the

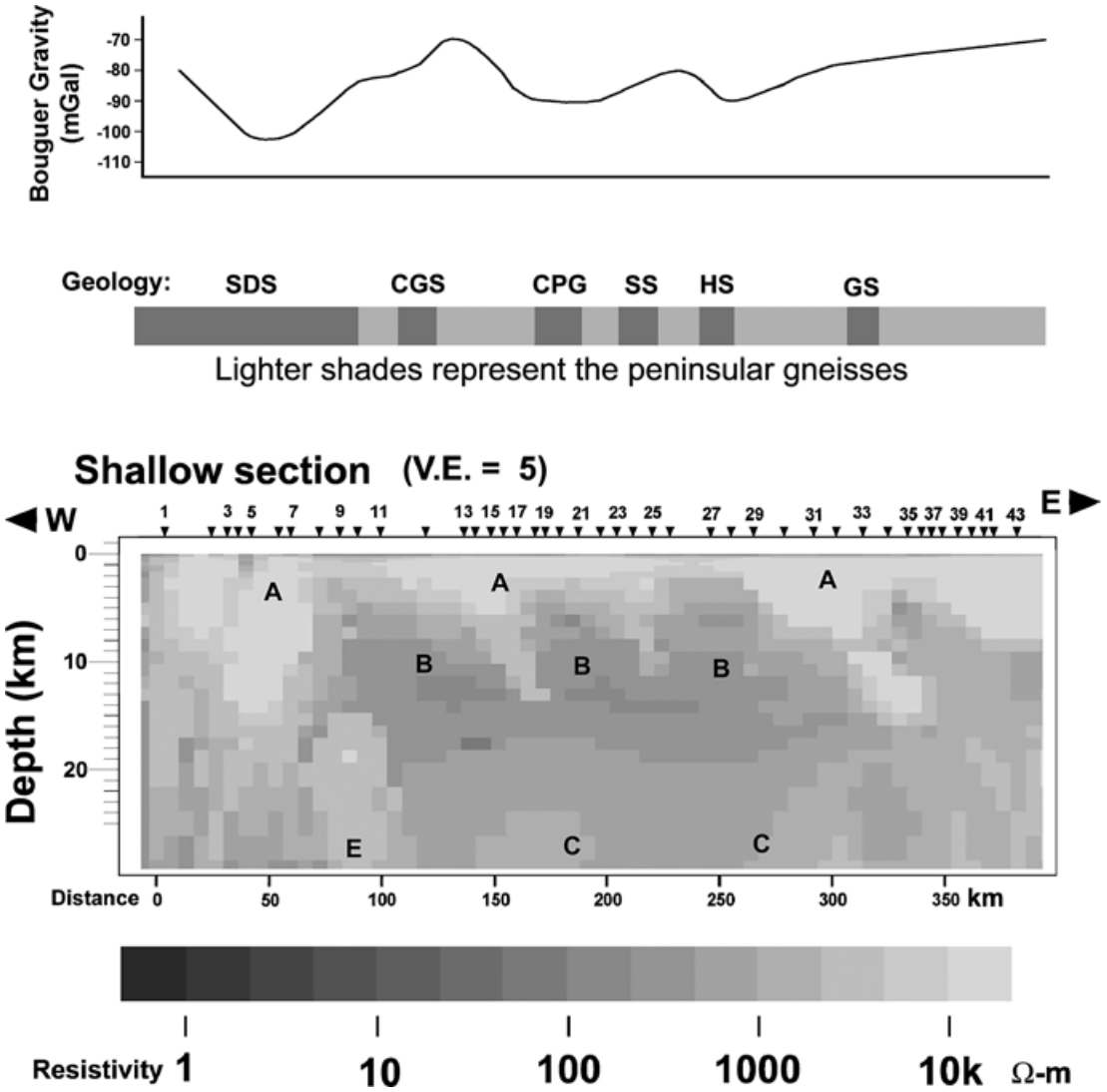


**Figure 7.** Geoelectric cross-section in the top 25 km. The Bouguer gravity variations along the MT profile are shown on the top part: SDS, Shimoga Dharwar schists; CGS, Chitradurga–Gadag schists; CPG, Closepet granites; SS, Sandur schists; HS, Hutti schists; GS, Gadwal schists.

different features in the responses was tested by studying the responses before and after removing them and retaining the other features in Figs 7 and 8 undisturbed. The response functions thus obtained are illustrated in Fig. 9. In all the cases to be discussed here, the difference in forward modelled phases (in both TE and TM modes) between the models before and after the removal of the feature were too small for any effective comparison and hence more emphasis is placed on the apparent resistivities and the shape of the curves in the discussion to follow.

As mentioned earlier, the survey region is located in close proximity to the Arabian Sea and the west coast is located at a distance of about 35 km to the west of station 1, as shown in Fig. 6. The effect of the sea was modelled by replacing the sea with a high resistivity of about 10 000 Ω m (resistivity of the feature A) and comparing the responses with those obtained from the original model. The maximum difference between the two models at any frequency in the TM phase was 0.5° at station 1, decreasing gradually to less than 0.1° at station 43. The decrease in the TE phase was about 0.2° at all stations. The TM-apparent resistivity at stations 1 and 2 (nearest to the coast) increased by about 10 per cent, which is small compared with the 30–40 per cent changes caused by the other structures, to be discussed later. Since these differences are very small they are not shown in Fig. 9. This observation indicates that the geoelectric structure was not affected by the effect of the coast. The Arabian Sea in the vicinity of the survey profile is rather shallow, with a depth increasing to about 100 m over a distance of 100 km. Furthermore, station 1 on the western part of the profile is about 30 km away from the coast (Fig. 6).

The geoelectric structure beneath stations 2–7 shows a monotonic decrease of resistivity with increasing depth, with high resistivity (A) extending up to a depth of about 30 km, decreasing to about 20 Ω m (G) at deeper levels. This behaviour is observed as the monotonically decreasing apparent resistivity and a high phase (>60°) at frequencies lower than 10 Hz, and is in good correspondence with the forward modelled values. In order to study the sensitivity of G, its resistivity was increased to 500 Ω m. The response functions thus obtained at stations 2, 3 and 5 (dashed line) are shown in Fig. 9, along with those before the replacement (solid lines) and the observed values. The observed apparent resistivity curves at some stations are shifted suitably to facilitate the comparison. The original curves are

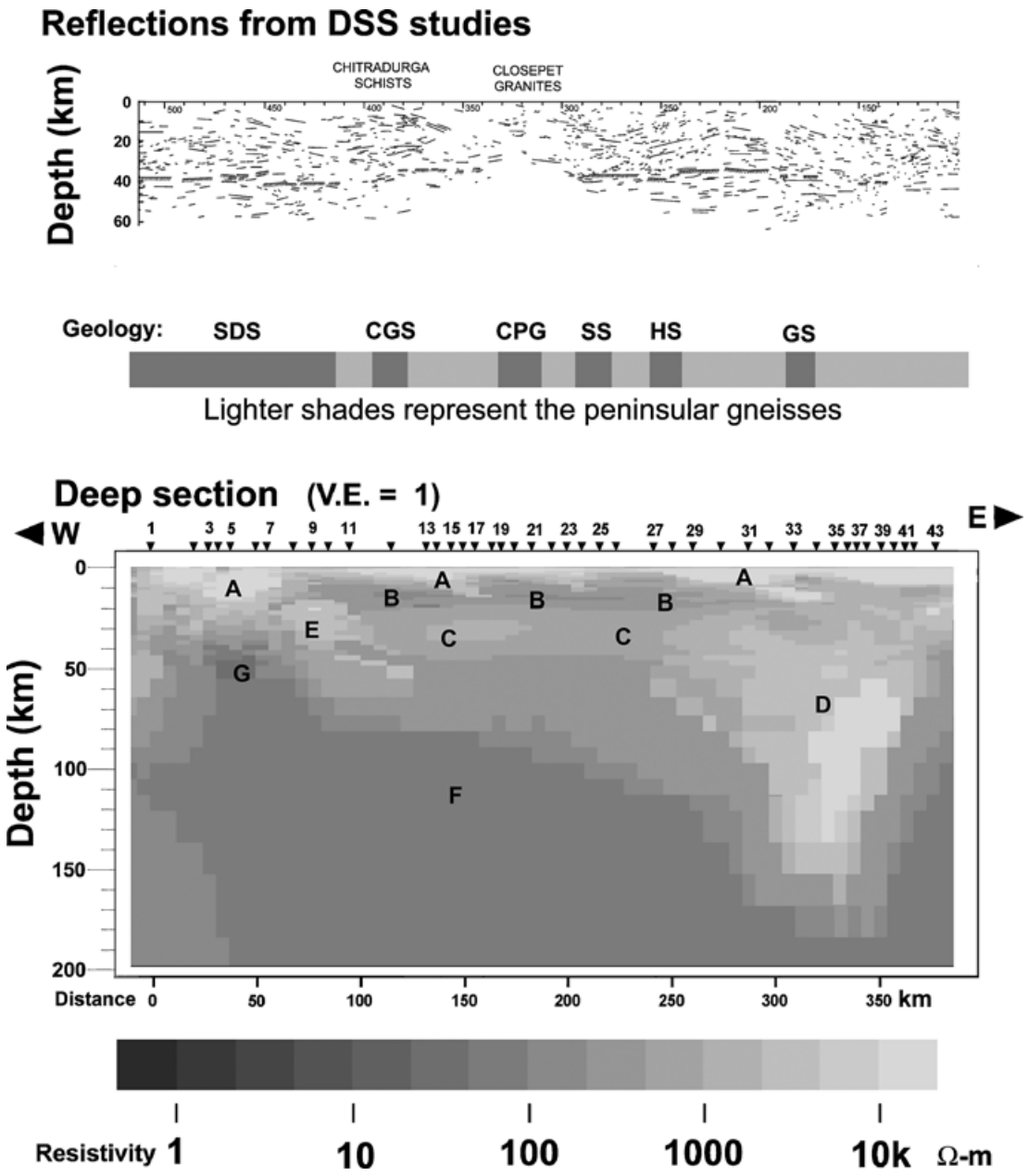


**Figure 8.** Deep geoelectric cross-section. Also shown on the top part are the seismic reflections obtained from the DSS studies along the Kavali–Udipi profile shown in Fig. 1, located about 200 km south of the MT profile: SDS, Shimoga–Dharwar schists; CGS, Chitradurga–Gadag schists; CPG, Closepet granites; SS, Sandur schists; HS, Hutti schists; GS, Gadwal schists.

shown (wherever possible) in a lighter shade of grey. The TE and TM phases in the two cases show a maximum difference of about 2° at frequencies lower than 1 Hz. The increase in the apparent resistivities in both the TE and TM modes is steeper at stations 2, 3 and 5 at frequencies lower than 0.1 Hz when the feature G is removed. When G is removed the difference between the two modes increases more rapidly with decreasing frequency than is required by the observed data. The observed and modelled (including G) responses show a more acceptable agreement. The dip in the apparent resistivities at frequencies between 1 and 0.1 Hz is more prominent at station 5 than at stations 2 and 3. This may be due to the proximity of station 5 to the high conductivity layer B.

A vertical resistivity contrast is detected near the western end of the profile beneath stations 1 and 2. Frequently such vertical contrasts are observed at the end stations in the 2-D geoelectric modelling as artefacts of the inversion. Station 1 is located in close proximity to the West Coast Fault (Fig. 1), which is a system of several subparallel fracture zones, and the possible presence of saline water may also have resulted in the observed resistivity structure here. As discussed earlier, the responses at station 2 are similar to those at stations 3 and 5 and other stations in the western block. However, striking dissimilarities exist from those at station 1, which is located about 20 km away from station 2. This dissimilar response is observed at only one station, and the hilly terrain and dense forest cover in this region do not permit additional station coverage here.

The feature B is reflected reasonably well in the response functions at stations 14 and 26, as the dip in the apparent resistivity near 0.1 Hz and the high phase 1–0.1 Hz. The increase in the apparent

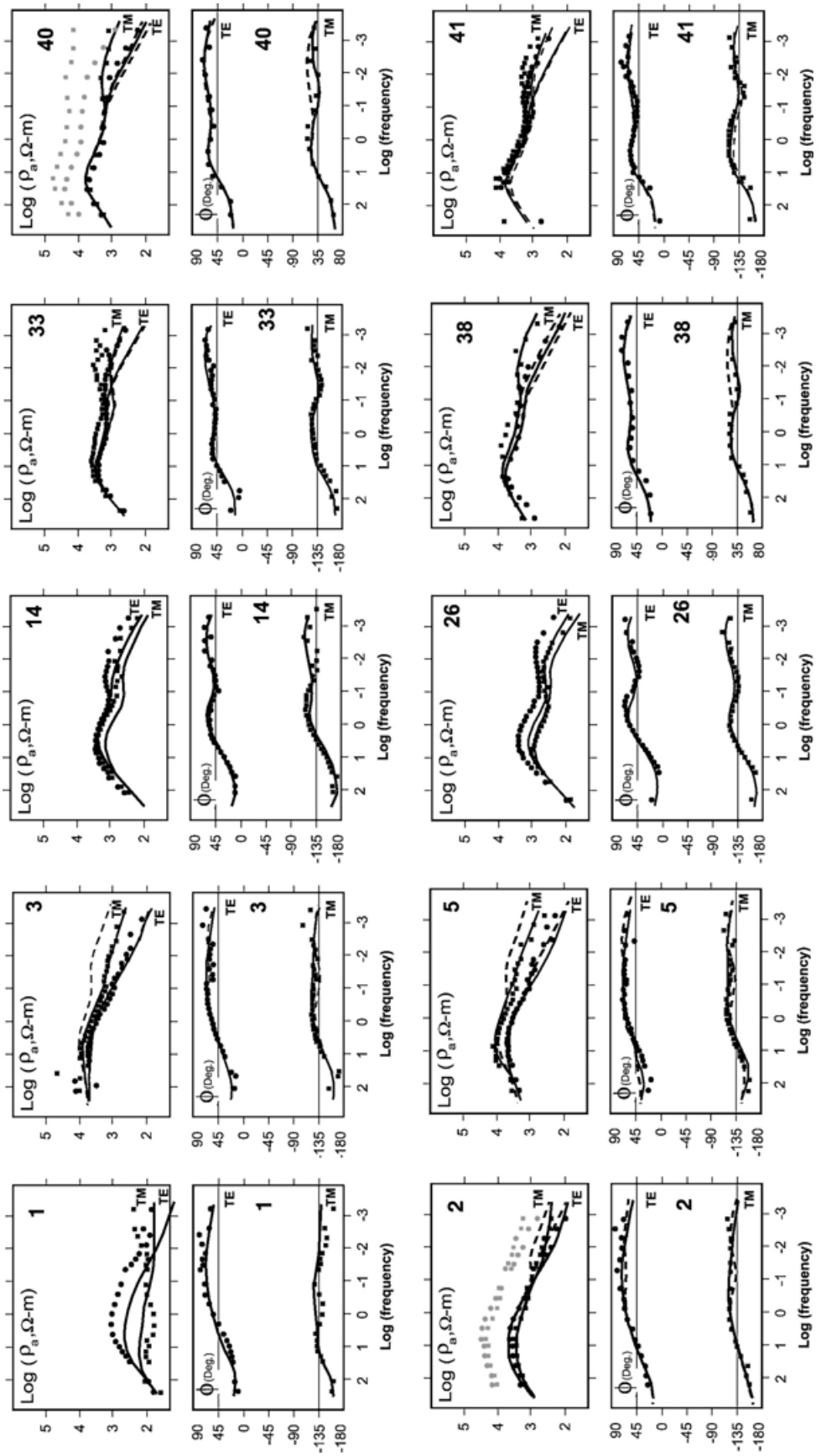


**Figure 9.** Observed and 2-D modelled response functions at some of the stations. The solid circles and squares denote the observed data in TE and TM modes respectively.

resistivity and dip in the phase at lower frequencies (0.1–0.01 Hz) confirm the high-resistivity layer C. Further east (stations 33 and 38), the dip in the mid-frequencies (1–0.1 Hz) in the response functions is relatively flat. This is clearly seen in the phase data at station 33 and is less obvious at station 41. This is indicative of the relatively weak vertical resistivity contrast offered by the deep crustal conductivity to the east of this station. No additional sensitivity studies were conducted on features B and C because the presence of these layered structures is adequately reflected in the observed and model responses.

The sensitivity of the high-resistivity feature D at depths ranging from 20–160 km was tested by removing it and extending the features C and F eastwards. The responses at stations 33, 38, 40 and 41, before and after this alteration are shown in Fig. 9 as solid and dashed lines respectively. The TE responses are insensitive to D but the TM responses are affected by its removal. The TM phase at frequencies between 0.1 and 0.001 Hz shows an increase, whereas the TM-apparent resistivities are high in the corresponding frequencies. Further more, the 2-D effect as observed from the difference in the TE and TM mode apparent resistivities decreases sharply at stations 33 and 41, on the conductive side of the lateral contrast offered by D. It seems that the feature D is necessary to explain the observed 2-D nature of the responses at low frequencies.

These sensitivity tests along with the overall rms misfit of 1.54 and the reasonable agreement between the observed and modelled phase pseudo-sections in Fig. 5(b) indicate an acceptable correspondence between the geoelectric cross-section and the observed responses. Some aspects of the structure could not be ascertained from the studies here. For example, are features C, D and E tectonically distinct or are they a single feature with differing resistivity and thickness? The case of features F and G is similar. Some possibilities will be discussed later.

## 7 INTERPRETATION OF THE GEOELECTRIC MODEL

The Archean crust is a mosaic of cratons which were once separated by oceans and later joined together along the suture zones during different geological times. The nature of the plate motions prior to 1000 Ma is still a topic of extensive debate. It is also uncertain whether the plate tectonic processes during the Archean were similar to those observed in the later periods, and whether the subsequent weathering and metamorphism can adequately explain the absence of ophiolites, flysch nappes, etc. in some of these sutures zones. Notwithstanding these controversies, the discussion here will be based on the merits of the observations as reported using different geophysical techniques, without making any specific presumptions about the temporal considerations.

### 7.1 Crustal structure of the Dharwar Craton

The geoelectric cross-section (Figs 7 and 8) shows the high-resistivity top layer (A), throughout the study region. The schist belts and the Closepet granitic intrusives embedded in the vast Peninsular gneissic complex cannot be easily distinguished from each other, because all these formations have similar resistivities. This layer has an uneven bottom and is generally about 3–5 km thick in the central and eastern part of the profile, east of station 9, with east-dipping wedges extending to a depth of about 12–18 km, indicative of thrust zones beneath the station sets 11–17, 21–25 and 27–33. In view of the fact that the predominantly Archean tectonic activities here may have been modified by the subsequent tectonic processes, it is appropriate to interpret the MT results jointly with the other geophysical and geological observations.

Although the bottom of the resistive bodies consists of well-determined parameter in the MT responses, its shape may not always be unequivocal. The layer A shows several east-dipping downward extensions at deeper levels. The phase pseudo-sections do show the extension of the high-resistivity feature; however, the east-dipping trend is not clear except in the TE phase between stations 21 and 27 in the frequency range between 10 and 0.1 Hz; they thus do not offer sufficient credence to the thrust hypothesis. This aspect may be more effectively resolved by comparing the crustal section with the seismic reflection patterns from the deep seismic sounding studies which are available along the Kavali–Udipi profile (top part of Fig. 8). The geological and tectonic setting over the two survey profiles is similar. Furthermore, all the geological features are reasonably parallel between the deep seismic sounding and MT profiles (Fig. 1). However, as mentioned earlier, the deep seismic sounding profile is located about 200 km south of the present study and hence the two data sets must be compared with caution. The deep geoelectric section is shown again in Fig. 10, with the seismic reflectors superimposed. The location of the Closepet granitic exposures reported from the geological studies is used here as the reference point to match the relative lateral positions of the MT and deep seismic sounding profiles and the sections have no vertical exaggeration.

Several east-dipping reflectors are present at shallow depth beneath station 12, which show a reasonable continuity up to a depth of about 20 km at station 15 and even beyond until they are intercepted by subhorizontal reflectors near the Moho beneath station 17. Further east, this line of reflectors continues up to station 23, where it is intercepted by the Moho. These seem to correspond to the bottom of the east-dipping resistive feature observed in the geoelectric section. There are very few reflectors at shallow depth to the immediate east up to station 23; most of them show horizontal to easterly dips. These observations indicate a deep-seated thrust along the resistive feature observed between stations 12 and 17, along which the East and West Dharwar blocks may have sutured, as shown in the geophysical cartoon (Fig. 12) to be discussed in detail later. The geoelectric structure and deep seismic reflections are shown in a light shade of grey in this figure. Some west-dipping reflectors at a depth of 30 km between stations 17 and 19 may be caused by the intrusion of the Closepet granites subsequent to the suturing of the two cratons. This discussion seems to provide adequate support for the existence of a suture along the Chitradurga–Gadag schist belts in the Dharwar Craton. Several thermotectonic events and vertical movements associated with the hotspot activities as well as the intrusion of granites subsequent to the suturing may have overprinted the signatures of this Archean suture.

The seismic reflections corresponding to the bottom of feature A beneath the station pairs 21 and 25 and 27 and 33 do offer some scattered support for the observed easterly dips in the resistivity pattern. However, they are more indicative of gentle anticlines rather than thrusts. This is surprising because gold mineralization is observed at several places along the Hutti and Kolar schist belts (Riyaz Ulla *et al.* 1996) and the working gold mine at Hutti is located near station 29 and another at Kolar. Both the Hutti and Kolar schists seem to be a part of a narrow, discontinuous and long schist belt. The presence of a thrust zone passing through the Hutti–Kolar region may be a more reasonable explanation for such localized gold mineralization over a linear belt than the crustal foldings indicated in the seismic reflectors. It thus seems more appropriate, albeit premature at this

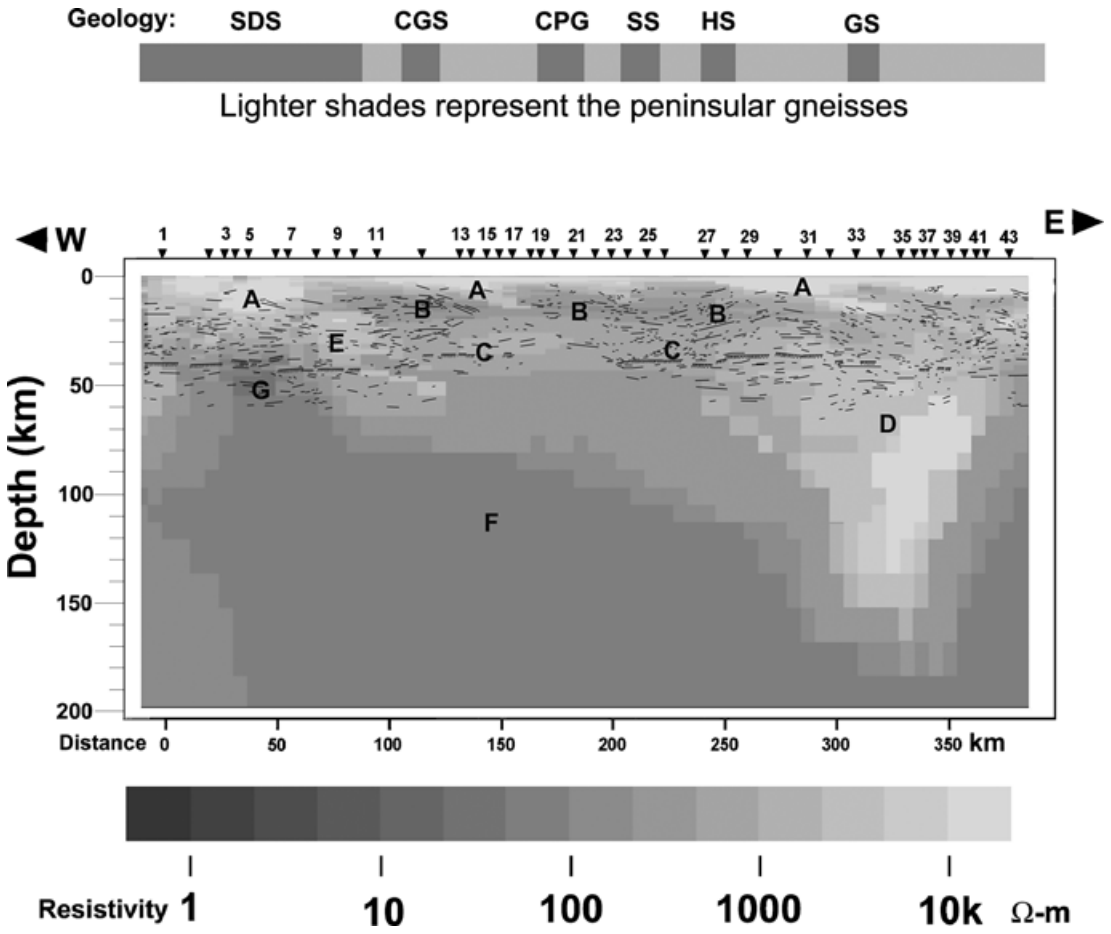


**Figure 10.** The geoelectric section and the seismic reflectors from the DSS section (Kavali–Udipi after Kaila *et al.* 1979) superimposed over each other for the sake of comparison. Vertical exaggeration is 1:1. SDS, Shimoga–Dharwar schists; CGS, Chitradurga–Gadag schists; CPG, Closepet granites; SS, Sandur schists; HS, Hutti schists; GS, Gadwal schists.

stage, to conjecture that this anticline over the Kavali–Udipi profile may have matured into a thrust zone on either side of it near the Hutti and Kolar schist belts.

The low-resistivity layer B has a conductance of about 100 S. A deep crustal conductor is normally present in some of the stable shield regions in several parts of the world (Jones 1992). However, the depth of 3–5 km to the top of this conductive layer is too shallow to be interpreted as the conventional deep crustal conductor in this cold crust with low heat flow values of about 41 mW $m^{-2}$. The gold mineralization in the Hutti and and Kolar schist belts in the east Dharwar Block mentioned earlier provide strong indications of carbon- and sulphur-rich fluids in the deep crust, which act as the conduits for such mineralization. It is thus inferred here that feature B is caused by either sulphur deposited in the form of pyrites or the presence of sulphur- and carbon-rich fluids, which may have risen through the fractured parts of the upper crust.

The high-resistivity layer A is thicker (30–40 km) in the western part of the profile between stations 1 and 5. An east-dipping low-resistivity feature is observed beneath station 1, and thus this may be related to the West Coast Fault (Fig. 1), which is in close proximity to this station, as discussed earlier.

The high-resistivity feature C, with a resistivity of about 1000 Ω m, in the central part of the profile corresponds to the lower crust. D seems to be the eastward continuation of C, but the depth of 160 km to which D extends is rather conspicuous. The subduction of the West Dharwar Craton proposed here, may only partly explain the thickening of the crustal block. The dips in the seismic reflectors also seem to indicate a possible thickening of the crustal block, with the depth of the Moho increasing by about 5 km beneath stations 32 and 34. However, the other causative factors leading to such anomalous thickening are not immediately apparent. It may, however, be noted that the sensitivity tests on D showed that this feature is invoked in the inversion scheme to account for the 2-D effects seen in the form of increasing difference between the TE and TM modes with decreasing frequency. Although the bottoms of the resistive layers are well-determined parameters in MT studies, the 2-D effects may have had a stronger influence on determining the depth to the bottom of D. Thus the depth extent of D may have been overestimated here. Some ambiguity also exists regarding the westward extension of C. Is E a westward continuation of C or is it the downward continuation of A? The seismic reflectors (Figs 8 and 10) indicate a synclinal pattern in this region. The crust is also thicker in this region, as is evident from the depression of the Moho by about 8 km beneath E. Thus it seems more likely that E is the continuation of A, the downward-dipping part of the (presumably thickened by compressive tectonics) West Dharwar Craton.

### 7.2 Lithospheric mantle

A thin lithosphere with a resistivity of about 500 Ω m beneath C is evident from the geoelectric cross-section (Fig. 8) and is underlain by the feature F, a low-resistivity asthenosphere. The presence of

about 1–3 per cent liquid phase at the lithosphere–asthenosphere boundary normally leads to low resistivity at this interface, which is delineated at depths of 80–100 km over the entire study area, except between stations 27 and 40 in the east block (discussed earlier) and stations 2 and 9 in the west block. The lateral spreading of the thermomechanical fluxes generated during the transit of the Indian Plate over the Reunion hotspot at the Cretaceous–Tertiary boundary as well as the resultant decompressional melting of the lithosphere due to the uplift of the Dharwar Craton caused by the hotspot may have generated a partial melt at this depth, leading to the low-resistivity feature (F) at the lithosphere–asthenosphere boundary.

The anomalous low resistivity of about 20 Ω m (G) has a width of about 50 km along the profile, and occurs at the depths greater than 40 km corresponding to the lithospheric mantle beneath stations 2 and 9 in the West Dharwar Block. Although the low resistivity at a depth of 40 km has the appearance of the upwelled part of the asthenosphere F, the causative factors leading to it may be different from those for the low-resistivity feature at the lithosphere–asthenosphere boundary. This is evident from the observed heat flow of 31 mW $m^{-2}$ in the western block, which is too low to offer any credence to the idea of upwelling in the lithosphere–asthenosphere boundary. Further more, this value is smaller than the heat flow of 40 mW $m^{-2}$ in the eastern block, where the low resistivity occurs at the greater depth of 80–100 km. Hence G is treated as a feature, distinct from the low-resistivity feature F.

Studies over two approximately east–west oriented MT profiles in the Deccan volcanic province (Gokarn *et al.* 2003), about 150 and 250 km north of the present study area, have shown similar low resistivities at depths of 50 and 90 km respectively near the west coast. This feature is shown in the plan view superposed over the Bouguer gravity map in Fig. 11. It is observed here that the low resistivity in the lithospheric mantle is a regional feature, extending over at least 250 km and perhaps even beyond in the offshore region of the Arabian Sea. Its southward extension is, however, yet to be ascertained. It is interesting to note that this low resistivity closely follows the trend of a major negative gravity anomaly of about −30 mGal over the surrounding area. Teleseismic studies (Srinagesh & Rai 1996) report higher seismic velocity in the lithospheric mantle of the west Dharwar Craton than in the eastern part, indicating high-density rocks at this depth. It may thus be inferred that the low-resistivity feature in the lithospheric mantle is associated with low surface heat flow of 30 mW $m^{-2}$, low gravity values and a high seismic velocity. The low heat flow and high seismic velocity are suggestive of the presence of high-density rocks corresponding to this low-resistivity zone and thus preclude the possibility of the partial melt causing the low resistivity G. The other possibilities will be examined in detail in the next section.

The feature D represents a high-resistivity body, extending in depth from 30 km to about 160 km. It is not clear whether this body is the eastward extension of C representing the thickening of the crustal block resulting from the compressive tectonic forces active during the Archean. It may also be the subducted west Dharwar crust, tectonically emplaced beneath the East Dharwar Block. However, the depth of 160 km to the bottom of D is rather large to be explained in terms of tectonic emplacement. As discussed earlier, D is required to account for the 2-D effects observed between stations 33 and 41. The depth to the bottom of this feature, although a well-determined parameter in MT studies, may have been overestimated in the studies here.

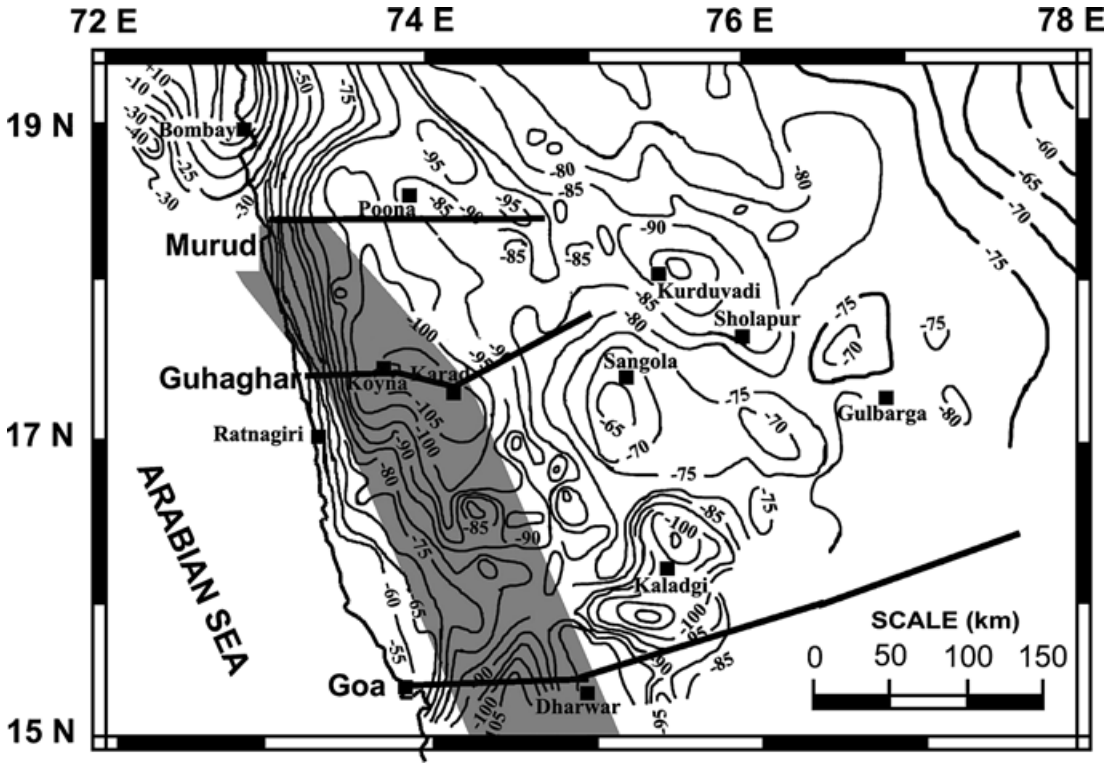


**Figure 11.** The low-resistivity feature in the lithospheric mantle in the plan view is shown in grey, superposed over the Bouguer gravity map of the Deccan volcanic province and the northern part of the Dharwar Craton. The eastern and western boundaries of the low resistivity are interpolated over the present study area and two additional profiles (marked using thick lines) over the Deccan volcanics. (After Gokarn *et al.* 2003).

## 8 DISCUSSION

The geoelectric cross-section shows several east-dipping high-resistivity bodies at shallow depth. The high-resistivity feature between stations 13 and 17 extends up to depth of about 15 km, corresponding to the bottom of the upper crust. The deep water marine sediments such as the greywackes, oceanic tholeiites, komatites etc., are known to be present along the Chitradurga–Gadag schist belts (Radhakrishna & Naqvi 1986), located on the top part of this high-resistivity feature. Based on these observations the east-dipping high-resistivity feature is conjectured to represent an intercratonic suture, along which the West Dharwar Block subducts beneath the east Dharwar Craton. Considering the Archean age of this suturing and also the subsequent tectonothermal events experienced in this region, the seismic reflectors give reasonable support for this hypothesis. This subduction may have caused the depression in the West Dharwar Block, which along with the accretionary wedge of the thrust may have formed the seat for the deposition of the schists during the Archean (2600 Ma). This hypothesis receives support from the observation that the Chitradurga–Gadag schist belts are narrow and extend to depth beyond 6 km whereas, the Shimoga–Dharwar schists to the west are deposited in a wide and shallow basin with a depth of less than 3 km (Subrahmanyam & Verma 1982). The exact location of the suture is not clear at present for several reasons. The sulphur- and carbon-rich fluids present in the deep crust may have risen to the shallow levels along the zone of weakness subsequent to the suturing, thus obliterating its signatures. The present results are indicative of a low-angle suture (20–30°) and thus its exact location on the surface may not be clearly defined. Perhaps a denser network of stations in and around the Chitradurga–Gadag schist belts will provide better constraints. Additional studies are planned in the Dharwar Craton along the deep seismic sounding profile and further south, which may help resolve this issue more effectively. These studies will also help in establishing the southward extension of the low resistivity in the lithospheric mantle.

The low resistivity in the lithospheric mantle is associated with low heat flow and high seismic velocity, which in turn implies a high density. As mentioned earlier, these observations preclude the possibility of partial melt. Similar low-resistivity features in the lithospheric mantle are observed in the Archean Slave Craton (Jones *et al.* 2001) and the Superior Craton (Craven *et al.* 2001) in northern Canada. The Slave Craton resembles the Dharwar Craton in several aspects. Perhaps the most striking similarity is the northwest–southeast trending subduction zone with an easterly dip near the Hackett River island arc (Bank *et al.* 2000). The seismic tomography in the Dharwar Craton (Srinagesh & Rai 1996) as well as in the Slave Craton (Bank *et al.* 2000) shows anomalous high velocity at depths corresponding to the low resistivity in the lithospheric mantle. The depth to the low-resistivity feature in the Slave Craton is about 80 km to the north of the Lac de Gras (Jones *et al.* 2001) and increases to about 180 km towards the south. In the Dharwar Craton and the adjoining Deccan volcanic province, the depth to the top of this low-resistivity feature increases from about 40 km over the present profile and to about 90 km beneath Murud (Fig. 11). Further north, the extension of this feature beneath the Arabian Sea is not known at present. The low-resistivity feature shows a sharp westward turn to its south and follows the westward trend of the Great Slave Lake shear. The high phase observed over the Big Lake suggests that the low resistivity in the mantle of the Slave Craton may have substantial spatial westward extension. In the Dharwar Craton, the westward as well as the southward extensions of this low-resistivity feature are not known at present.

The factors leading to the low electrical resistivity in the lithospheric mantle may differ from those in the crust because of the differing pressure and temperature conditions. As discussed earlier, a partial melt is ruled out on heat flow as well as density considerations. The presence of sulphides is well established in the east Dharwar crust from the observed gold mineralization as well as the observed low resistivity B in the mid-crustal region. However, since west Dharwar Craton was a distinct cratonic block prior to the collision, the mobile sulphides in the lithosphere (Alard *et al.* 2000) may not explain the low resistivity, unless similar conditions existed in the west Dharwar Craton prior to the collision. The graphite, which is the stable phase of carbon at depths of less than 150 km, seems to be the likely cause of this low resistivity. In spite of the fact that the Dharwar is an Archean craton, where the aqueous fluids have had sufficient time to escape from the crust and mantle, the distinct possibility exists that such fluids may have been replenished during the passage of this region over the Reunion hotspot, in the waning phase of its Tertiary outburst. Thus a low resistivity due to aqueous fluids is a distinct possibility here.

Based on the foregoing discussion, a first-order crustal evolutionary model is proposed here as shown in Fig. 12. The East and West Dharwar blocks were distinct cratons with an intervening sea (Fig. 12a) which moved towards each other, and the ensuing compressional tectonic forces may have caused intracratonic thrusts in the East Dharwar Craton. The accretionary wedges of these thrusts formed the seat of deposition for the older schist belts (the Hutti–Kolar and the Sandur schists). The subsequent compression resulted in the formation of the suture zone, along which the West Dharwar Craton subducted beneath its eastern counterpart and younger schist belts (Chitradurga–Gadag and Shimoga–Dharwar) were deposited in the accretionary wedge of the intercratonic suture during the Late Archean (2600 Ma), as shown in Fig. 12(b). Subsequent intrusion of the Closepet granites and weathering and erosion may have resulted in the present-day crust, as shown in Fig. 12(c). Here the geoelectric cross-section as well as the seismic reflectors are superimposed over the interpreted section for the sake of comparison.

The differences in the crustal evolutionary processes reported by several authors are also explained by the model proposed here. Perhaps the most significant observation is the lateral resistivity contrasts in the mantle depth. This can only be explained by the collision hypothesis presented here. The east Dharwar crust is dotted with several granitic intrusives, the Closepet granites being the most prominent among them, which are not observed in the West Dharwar Craton. Gupta *et al.* (1991) have suggested different magmatic processes in the West and East Dharwar blocks, based on the observation that the gneisses in west Dharwar have a tonalitic character, where as those in the eastern block are rich in granitic intrusions. Subrahmanyam & Verma (1982) observed an anomalous long-period gravity low in the West Dharwar Craton, which could be explained by a low-density body at the mantle depth, where as the seismic tomography studies have delineated a high density at this depth.

## 9 CONCLUSIONS

The geoelectric structure in the Dharwar Craton is suggestive of several east-dipping resistivity features which may have resulted from intense compressive tectonic activity. In view of the possible overprinting of the signatures of these Archean events by subsequent

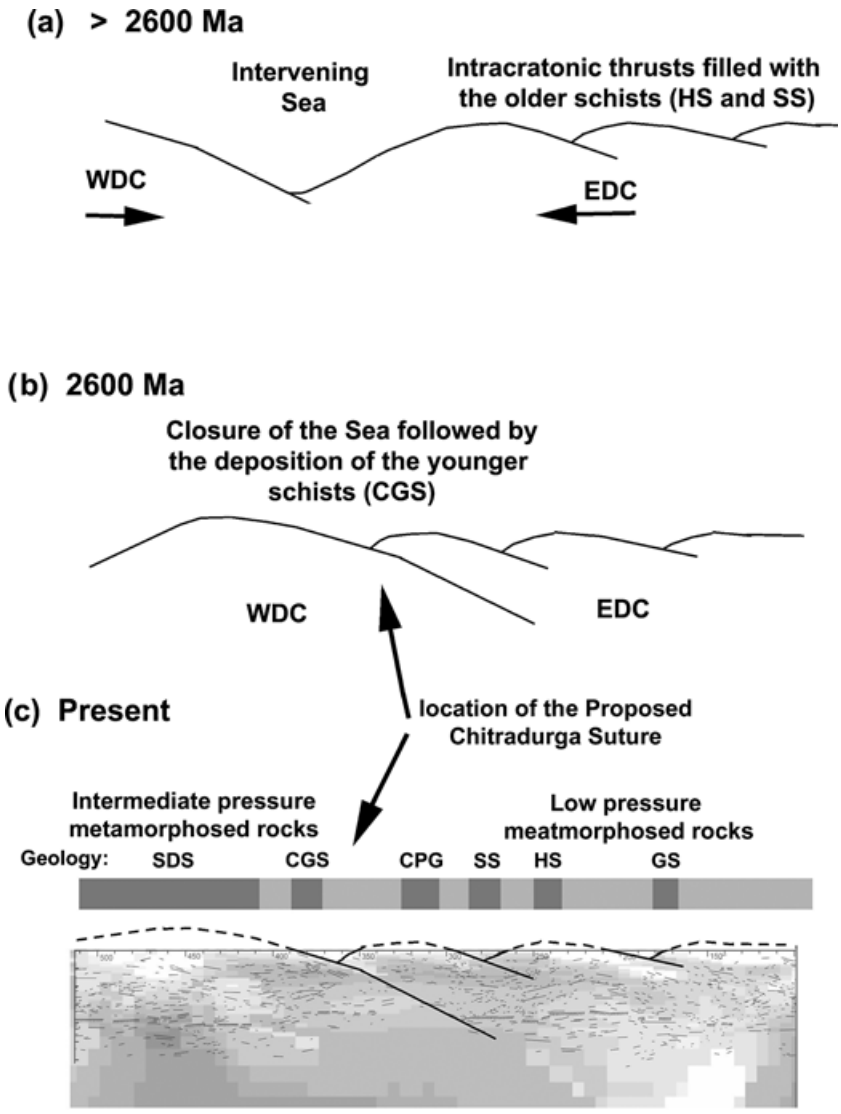


**Figure 12.** Proposed stages in the crustal evolution of the Dharwar Craton: WDC, West Dharwar Craton; EDC, East Dharwar Craton; HS, Hutti Schists; SS, Sandur schists; CGS, Chitradurga–Gadag schists; SDS, Shimoga–Dharwar schists; CPG, Closepet granites; GS, Gadwal schists.

events such as thermotectonic activity throughout the Precambrian (Mukhopadhyay 1986) and vertical block movements related to the passage of this region over the Reunion hotspot, the electrical structure is interpreted jointly with the other available geophysical and geological results. A suture zone along the Chitradurga–Gadag schist belt is conjectured, along which the West Dharwar Craton subducts eastwards beneath the East Dharwar Block at an angle of about 30°. This is based on the east-dipping high resistivity beneath stations 11 and 17 coinciding with the greywackes (Radhakrishna & Naqvi 1986) and other evidence of rocks of oceanic origin as well as some evidence from the seismic reflectors (Fig. 8). The present studies also indicate that the accretionary wedge of this east-dipping thrust and depressed part of the subducting West Dharwar Craton may have formed the seat of the deposition for the younger schist belts in Chitradurga–Gadag and the Shimoga–Dharwar regions) during the Late Archean. The age of this suture pre-dates the deposition of these schists and thus it may have occurred prior to the Late Archean (2600 Ma). A detailed determination of the ages of different rock formations in the Dharwar region may be useful in constraining the dates of the other events.

Although another intracratonic thrust is delineated near the location of the gold mineralization along the Hutti–Kolar schist belts, which seem to be a part of a single discontinuous schist belt, the seismic reflectors obtained from deep seismic sounding studies are more indicative of an anticline. Normally thrust zones are more appropriate for understanding gold mineralization over such narrow and long regions because they facilitate the uprising of carbon- and sulphur-bearing fluids which act as the conduits for the gold mineralization. The deep seismic sounding profile is located about 200 km south of the MT profile. Perhaps the anticline there may have matured into a thrust zone to the north, near the Hutti schists, which is delineated here at station 29 and (possibly) to the south near the Kolar schists.

A low resistivity is delineated at depth of 50 km and beyond corresponding to the lithospheric mantle. The exact cause of this low resistivity is not immediately apparent. The low heat flow and high seismic velocity in this region do not support the possibility of partial melting due to the uprising of mantle material. This low resistivity was thus attributed to the presence of aqueous fluids generated during the passage of the West Dharwar Block over the Reunion hotspot

in the waning phase of its Tertiary outburst. However, the possibility of the presence of carbon in the form of grain boundary graphite, as well as the other mechanisms of electronic conductivity which are generally expected at depths of 50 km and beyond corresponding to the lithospheric mantle, may also provide an alternative explanation for the observed low resistivity. Magnetotelluric studies in the Deccan volcanic province north of the present study area also observe a similar low resistivity in the lithospheric mantle, indicating that this is a regional feature with a spatial extent of at least about 250 km.

## ACKNOWLEDGMENTS

This work was carried out under sponsorship and funding by the Department of Science and Technology (DST), Government of India, under the Deep Continental Studies programme (project no ES/16/052/96). Heart-felt thanks are due to Dr K. R. Gupta for his cooperation. Thanks to Mr C. Selvaraj for his help and enthusiastic participation in the field work. We express our heart-felt thanks to Prof. B. P. Singh, Shri D. N. Avasthi and Dr U. Raval for several useful discussions and encouragement. Grateful thanks to Dr Alan Jones and Mr Gary McNeice for the strike determination programme. We are grateful to Dr Alan Jones and Dr Ute Weckman for the patient reading, critical review and extremely useful comments.

## REFERENCES

Alard, O., Griffin, W.L., Lorand, J.P., Jackson, S.E. & O'Reilly, S.Y., 2000. Non-chondritic distribution of the highly siderophile elements in mantle sulphides, *Nature,* **407**, 891–894.

Bank, C.-G., Bostock, M.G., Ellis, R.M. & Cassidy, J.F., 2000. Reconnaissance teleseismic study of the upper mantle and transition zone beneath the Archean Slave craton in NW Canada, *Tectonophysics,* **319**, 151–166.

Boger, S.D., Carson, C.J., Fanning, C.M., Hergt, J.M., Wilson, C.J.L. & Woodhead, J.D., 2002. Pan-African intraplate deformation in the northern Prince Charles Mountains, east Antarctica, *Earth planet. Sci. Lett.,* **195**, 195–210.

Cox, K.G., 1989. The role of mantle plumes in the development of continental drainage patterns, *Nature,* **342**, 873–877.

Craven, J.A., Kurtz, R.D., Boerner, D.E., Skulski, T., Spratt, J., Ferguson, L.J. Wu, X. & Bailey, R.C., 2001. Conductivity of western Superior Province upper mantle in northwestern Ontario, *Geological Survey of Canada Current Research*, 2001-E6.

Eremenko, N.A. & Negi, B.S., 1968. *Tectonic Map of India,* Publ: Oil and Natural Gas Corporation Ltd. (formerly the Oil and Natural Gas Commission).

Gokarn, S.G., Gupta, G., Rao, C.K. & Selvaraj, C., 2003. Some interesting observations on the tectonics in the Deccan Volcanic province observed from magnetotelluric studies, *J. Virtual Explorer, in press.*

Groom, R.W. & Bailey, R.C., 1989. Decomposition of the magnetotelluric impedance tensor in the presence of local three-dimensional galvanic distortions, *J. geophys. Res.,* **94**, 1913–1925.

Groom, R.W., Kurtz, R.D., Jones, A.G., & Boerner, D.E., 1993. A quantitative methodology for determining the dimensionality of conductivity structure from magnetotelluric data, *Geophys. J. Int.,* **115**, 1095–1118.

Gupta, M.L., Sundar, A. & Sharma, S.R., 1991. Heat flow and heat generation in the Archean Dharwar cratons and its implications for the Southern Indian Shield geotherm and lithospheric thickness, *Tectonophysics,* **194**, 107–122.

Gupta, S., Rai, S.S., Prakasam, K.S., Srinagesh, D., Bansak, B.K., Chadha, R.K., Pristley, K. & Gaur, V.K., 2003. The nature of the crust in southern India: implications for Precambrian evolution, *Geophys. Res. Lett.,* **30**, 1.1–1.4.

Harikumar, P., Rajaram, M., & Balakrishnan, T.S., 2000. Aeromagnetic study of peninsular India, *Proc. Indian Acad. Sci. (Earth Planet. Sci.),* **109**, 381–391.

Jones, A.G., 1992. Electrical properties of the lower continental crust, in, *Continental Lower Crust,* pp. 81–144, eds Fountain, D.M., Arculus, R. & Kay, R.W., Elsevier, Amsterdam.

Jones, A.G. & Dumas, I., 1993. Electromagnetic images of a volcanic zone., *Phys. Earth planet. Inter.,* **81**, 289–314.

Jones, A.G., Ferguson, I.J., Chave, A.D., Evans, R.L. & McNeice, G.W., 2001. Electrical lithosphere of the Slave craton, *Geology,* **29**, 423–426.

Kaila, K.L., Roy Choudhury, K., Reddy, P.R., Krishna, V.G., Narayan, H., Subbotin, S.I., Sollogub, V.B. & Chekunov, T.V., 1979. Crustal structure along Kavali-Udipi profile in the Indian peninsular shield from deep seismic sounding, *J. Geol. Soc. India,* **20**, 307–333.

Kumar, A., Pande, K., Venkatesan, T.R. & Bhaskar Rao, Y.J., 2001. The Karnataka late Cretaceous dykes as products of the Marion hotspot at the Madagascar–India breakup event; evidence from $^{40}$Ar-$^{39}$Ar geochronology and geochemistry, *Geophys. Res. Lett.,* **28**, 2715–2718.

McNeice, G.W. & Jones, A.G., 2001. Multisite, multifrequency tensor decomposition of magnetotelluric data, *Geophysics,* **66**, 158–173.

Mukhopadhyay, D., 1986. Structural pattern in the Dharwar craton, *J. Geol.,* **94**, 167–186.

Narayanaswami, S., 1975. Proposal for charnokite-khondalite system in the Archean shield of peninsular India, *Geol. Surv. India, Misc. Publ.,* **23**, 1–16.

Qureshy, M.M., Brahmam, N.K., Verma, R.K., Bhalla, M.S., Garde, S.C., Divakar Rao, V. & Naqvi, S.M., 1967. Geological, geochemical and geophysical studies along 14th parallel in Mysore, *Proc. Symp. Upper Mantle Project, Hyderabad, India, 4–8 January 1967,* pp. 211–225.Geophysical Research Board & National Geophysical Research Institute, Hyderabad, India.

Radhakrishna, B.P., 1984. Archean granite-greenstone terrain of the south Indian shield, *Mem. Geol. Soc. India,* **4**, 1–46.

Radhakrishna, B.P. & Naqvi, S.M., 1986. Precambrian continental crust of India and its evolution, *J. Geol.,* **94**, 145–166.

Ramam, P.K. & Murty, V.N., 1997. *Geology of Andhra Pradesh,* Geological Society of India, Bangalore, India.

Raval, U. & Veeraswamy, K., 2000. Radial and linear modes of interaction between mantle plume and continental lithosphere: a case study from western India, *J. Geol. Soc. India,* **56**, 525–536.

Riyaz Ulla, M.S., Pathan, A.M. & Maaskant, P., 1996. The characterization of metamorphic facies of metabasalts in the Hutti greenstone belts, *J. Geol. Soc. India,* **47**, 547–554.

Rodi, W. & Mackie, R.L., 2001. Nonlinear conjugate gradients algorithm for 2D magnetotelluric inversions, *Geophysics,* **66**, 174–187.

Roy, S. & Rao, R.U.M., 2000. Heat flow in the Indian shield, *J. geophys. Res.,* **105**(B11), 25 587–25 604.

Srinagesh, D. & Rai, S.S., 1996. Teleseismic tomographic evidence for contrasting crust and upper mantles in south Indian Archean terrains, *Phys. Earth. planet. Inter.,* **97**, 27–41.

Subrahmanyam, C. & Verma, R.K., 1982. Gravity interpretation of Dharwar greenstone-gneiss-granite terrain in the south Indian shield, its geological implications, *Tectonophysics,* **84**, 225–245.

Swami Nath, J., Ramakrishnan, M. & Vishwanatha, M.N., 1976. Dharwar stratigraphic model and Karnataka craton evolution, *Rec. Geol. Surv. India,* **107**, 149–175.

Wight, D.E. & Bostick, F.X., 1980. Cascade decimation—a technique for real time estimation of power spectra, *Proc. IEEE Int. Conf. Acoustic, Speech Signal Processing, Denver, Colorado, 9–11 April,* 626–629. Institute of electrical and electronic engineers, New York, USA.